Indian Geotech J
https://doi.org/10.1007/s40098-024-01043-z

ORIGINAL PAPER

Study on Seepage and Stability of Soft Rock Slope with Fissures Under Extreme Rainfall

Dinggui Hou[1] · Yunze Ma[1] · Yunying Zhou[1] · Xinyu Zheng[1] · Zeya Du[1]

Received: 28 September 2023 / Accepted: 26 July 2024

Abstract Extreme rainfall can lead to instability of fissured soft rock slopes. In this study, under the background of Nanfen open-pit mine slope, the seepage characteristics of slope fissured rock mass under extreme rainfall and the influence of seepage and rock softening factors on slope stability were investigated through numerical simulation. The pore water pressure and safety factor in the slope without drainage measures and with drainage holes were compared. As revealed by the results, the fissure depth was positively correlated with the rainfall infiltration depth and range, the fissure angle was negatively correlated with the rainfall infiltration depth, the fissure spacing was negatively correlated with the rainfall infiltration range and the size of the slope saturated area, and the permeability coefficient ratio was positively correlated with the rainfall vertical permeability. In the early stage of extreme rainfall, the slope stability was mainly reduced due to fissure seepage, with the duration of rainfall, the influence of softening of soft rock on the slope safety factor gradually increased, and at the end of rainfall, the decrease of fissure seepage and rock softening factors on the slope safety factor was 22.3% and 24.2%, respectively. In the process of extreme rainfall, the safety factor of slope could be kept above 1.11 by using inclined drainage hole slope drainage, which was 21.6% higher than that without drainage hole. The research results can provide a reference for the stability analysis and landslide control of soft rock slope with fissure development under extreme rainfall conditions.

Keywords Rock slope · Fissure · Extreme rainfall · Slope stability · Numerical simulation

Introduction

Under the condition of heavy rainfall, the infiltration of fissured soft rock slope and the softening of rock mass caused by rainfall are the difficulties in the field of landslide disaster research [1, 2]. Rainwater infiltration will cause the change of pore water pressure field and reduce the stability of slope [3, 4], and the variation of pore water pressure field of fissured rock mass is affected by fissure depth, fissure angle, fissure spacing and permeability coefficient ratio [5–7]. For soft rock slope, the softening effect of soft rock in water is also an important cause of slope disaster [8]. Therefore, it is necessary to study the fissure seepage and softening characteristics of soft rock slope under rainfall.

Rainfall is an important factor inducing slope instability; many scholars have studied the rainfall infiltration of slope [9–14]. Zhou et al. [15] established the lower-limit analysis model of slope stability under unsaturated seepage. Zhang et al. [16] found that the deformation of fill slopes induced by short-term continuous rainfall has shallow intermittent and sudden damage. Pedroso et al. [17] proposed a simple and effective method to realize the boundary conditions of finite element seepage surface. Zuo et al. [18] obtained the variation law of slope volume water content, pore water pressure and soil suction with rainfall infiltration. Shi et al. [19] explored the water content distribution of soil slope under the condition of rainfall infiltration. Deng et al. [20] introduced Monte Carlo method into the early warning and prediction of rain-induced landslides. Chang et al. [21] explained the failure mechanisms of each failure stage based on the changes in the hydrological and mechanical

✉ Dinggui Hou
houdinggui@126.com

[1] Construction Engineering Department, North China Institute of Aerospace Engineering, Langfang 065000, China

Published online: 02 August 2024

conditions of the slope with the infiltration of rainwater. Liu et al. [22] proposed a slope reliability analysis method considering rainfall. Tian et al. [23] proposed a two-dimensional simplified numerical method that considers the impact of runoff recharge on landslide infiltration. Bandara et al. [24] proposed a simulation method of unsaturated slope landslide under rainfall infiltration. Ma et al. [25] found that the relationship between rainfall intensity and the saturated permeability coefficient of soil slopes determines the distribution characteristics of pore water pressure. Long et al. [26] carried out the dry wet cycle experiment of red clay slope under different rainfall intensity.

The existence of fissures will have an important impact on the seepage field of rock and soil [27, 28], and a lot of research on fissure seepage has been carried out. Duan et al. [29] studied the seepage characteristics of single fissured limestone under water rock interaction. Park et al. [30] found that the generation of local flow circulation is due to the interaction between the cross geometry and the corresponding boundary conditions of flow along the crack boundary. Sheng et al. [31] explored the permeability characteristics of limestone fissures under the condition of temperature change. Zhang et al. [32] established a rock mass strength degradation model and calculated and analyzed it in combination with the reservoir bank slope. Hou et al. [33] simulated the transient water migration of slope under different fissure depths. Leng et al. [34] discussed the role of rainfall and traffic load in the process of slope fissure expansion and deformation development. Zhang et al. [35] discussed the research progress of deformation and failure of hydraulic coupling fissured rock mass. Guo et al. [36] studied the seepage characteristics of fissured marble. Liu et al. [37] found that under shear load, the permeability of cracks decreases with the increase of shear stress before shear action. Xiong et al. [38] conducted experimental and numerical study on single fissure seepage. Zhang et al. [39] conducted experiments on seepage characteristics of red sandstone with different damage degrees. Valko et al. [40] used the continuum damage mechanics method to simulate the fluid driven fracture propagation in the process of large-scale hydraulic fracturing of oil and gas reservoirs. Yan et al. [41] found that the infiltration rate of rainwater was higher than that of non-fissured slope due to the formation of centralized infiltration points at the fissures.

Due to the high complexity of the coupling mechanism between water and rock mass of soft rock, the analysis of rainfall seepage and rock mass softening of soft rock slope is still in the exploratory stage [42]. Bai et al. [43] conducted a model test on the catastrophic process of landslide geological disasters under the action of rainfall. Yang et al. [44] obtained the process of thick soft rock failure under rainfall conditions. Xie et al. [45] found the microstructure characteristics of mudstone under the long-term action of water. Ji et al. [46] analyzed the microstructure evolution of weakly cemented sandstone in the process of softening in water. Jiang et al. [47] found that as the water content decreased, the total energy absorbed by the mudstone increased. Picarelli et al. [48] found that even small details can affect the movement pattern of flow like landslides. Xin et al. [49] analyzed the influence of groundwater activities on soft rock landslide.

Rainfall is an important inducement to induce landslide disasters; especially under extreme rainfall conditions, slope cracks cause changes in seepage field and lead to instability disasters of soft rock slope, which cannot be ignored. In view of this, the numerical simulation method was used to study the rainwater infiltration process of fissured slope under extreme rainfall, and the mechanism of instability of soft rock slope induced by extreme rainfall was discussed. The research results can provide reference for the stability analysis and landslide disaster treatment of similar fissured soft rock slope.

Project Profile

Nanfen open-pit mine is located in Liaoning Province (Fig. 1), China. The mine was completed and put into operation in 1957; it was the largest single open-pit iron mine in Asia. In September 2004, phase III and phase IV mining design was carried out to increase the annual mining stone to 12 million tons and the annual stripping rock to 84 million tons.

Engineering Geology

The landform of the mining area is eroded medium high mountain landform, which is mainly composed of metamorphic rock strata. After years of open-pit mining activities, the footwall slope of open-pit mine has been formed (Fig. 2b). Under the influence of mining, the footwall slope had developed fissures, high rock permeability and low overall strength. The landslide area is located on the footwall slope of Nanfen open-pit mine, with an elevation of 370–622 m. After many landslides, zone I, II and III landslide masses are formed (Site 1 and Site 2 in Fig. 2), and the area distribution of landslide mass in the study area is shown in Fig. 2a.

The mining area is located in the north temperate monsoon climate area. The annual average rainfall is 880 mm, the maximum daily rainfall is 274 mm, the rainfall is concentrated from June to September, and the annual average evaporation is 1729 mm. The statistics of distribution of monthly average rainfall from 2010 to 2012 are shown in Fig. 3; it can be seen that the maximum rainfall month is August, and the monthly rainfall reaches 361 mm.

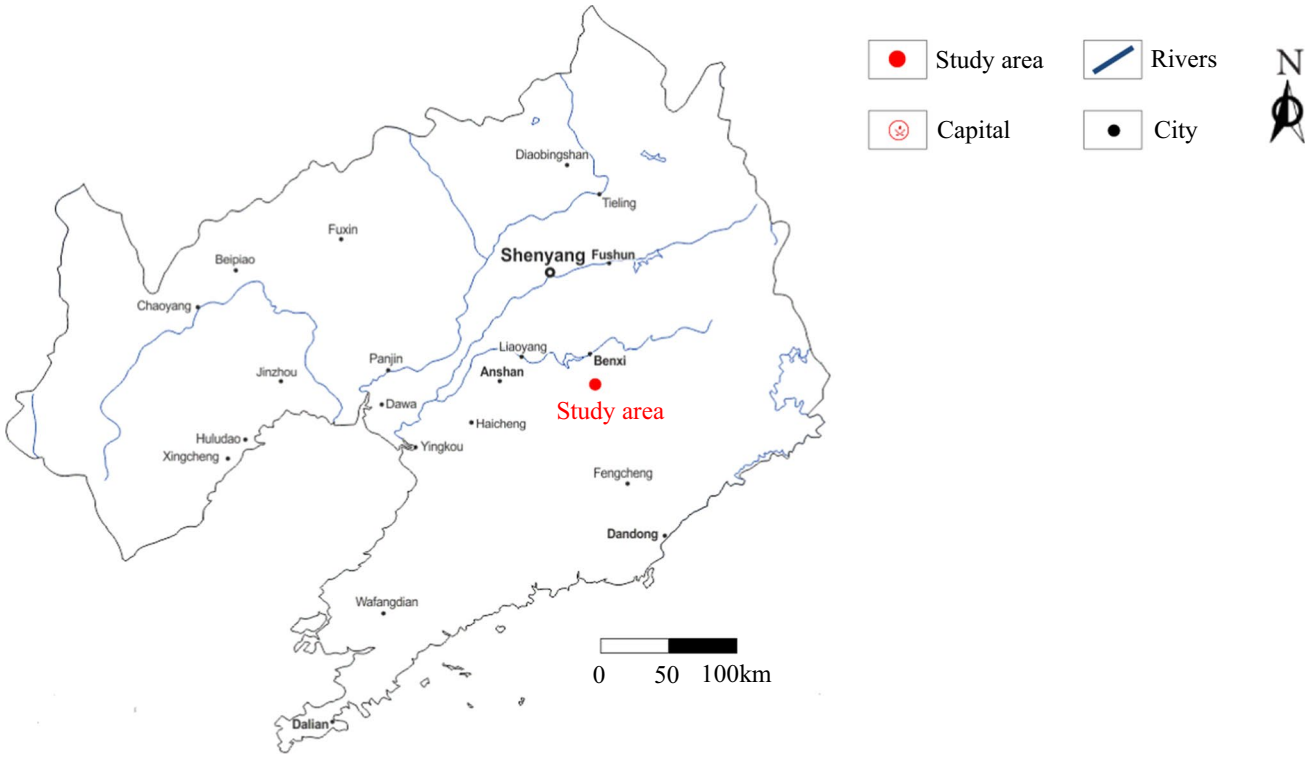

Fig. 1 Location map of the study area and its nearby cities

Rock Mass Properties

Through our geological radar geophysical prospecting and borehole coring, we can conclude that the slope is composed of chlorite amphibolite in the upper part and iron-bearing chlorite quartzite rock in the deep part. Under the action of weathering, rainfall, blasting, landslide and other factors, the slope has formed four rock stratum: fissure development area, fissure relatively developed area, and chlorite amphibolite rock and iron-bearing chlorite quartzite rock in the fissure undeveloped area. 2–5 m thick loose deposits formed by rock weathering are widely distributed in the fissure development area, the fissure relatively developed area is composed of 5–10 m thick broken rock mass and weathered soil mass, and the fissure undeveloped area is relatively complete chlorite amphibolite. The engineering geological profile of footwall slope of Nanfen open-pit mine is shown in Fig. 4. The mechanical parameters of slope stratum are shown in Table 3.

Brief History of Landslide Disaster

Before 2010, there were three major landslides on the footwall slope of Nanfen open-pit mine. In July 2000, a landslide occurred on the 370 m to 622 m bench, with an inclined length of 252 m, a width of 250 m and a volume of 5.2×10^5 m^3. In August 2008, a landslide occurred on the 394–526 m bench, with a length of about 130 m and a width of about 200 m. In June 2009, a large-scale potential collapse body appeared on the 430–526 m slope platform. Since 2010, with the mining of ore resources and slope expansion, many geological disasters such as tension fissures and collapse have occurred at 310–390 m steps, and the unstable area of the slope has been transferred to 310–390 m steps.

A large number of loose bodies have accumulated on the slope surface, increasing the sliding force of rock mass; at the same time, mining and expanding the slope toe will reduce the anti-sliding force of rock mass. The loose accumulation and rock mass fissures enhance rainfall infiltration, the chlorite soft rock on the potential sliding surface softens with water, and the rock mass strength decreases and further reduces the slope stability.

Real-time monitoring of rainfall and footwall slope landslide in the mining area, and statistics of rainfall and footwall slope landslides in Nanfen open-pit mine are shown in Table 1. The statistics show that landslides usually occur after rainfall; especially in August with frequent heavy rainfall (Site 3 and Site 4 in Fig. 2), the number of landslides increases significantly, which indicates that rainfall is an important factor of footwall slope landslide.

Extreme rainfall will change the distribution of pore water pressure in rock and soil, soften soft rock, and

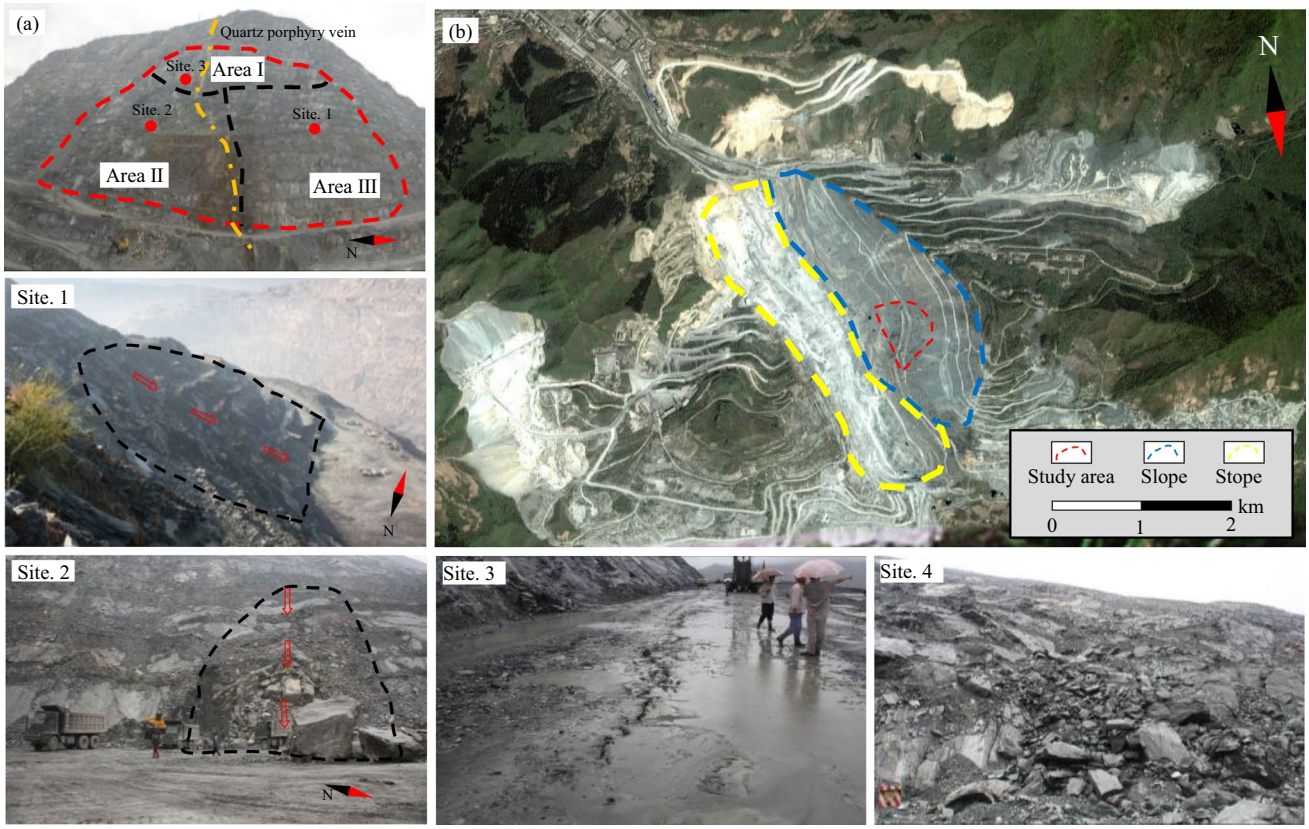

Fig. 2 Field observations of the slope: **a** area I distribution of landslide mass in the study area; Site 1: landslide in area II; Site 2: landslide in area III; Site3: rainfall induced slope step fissures; Site 4: rainfall induced small landslide; **b** Footwall slope of Nanfen open-pit mine

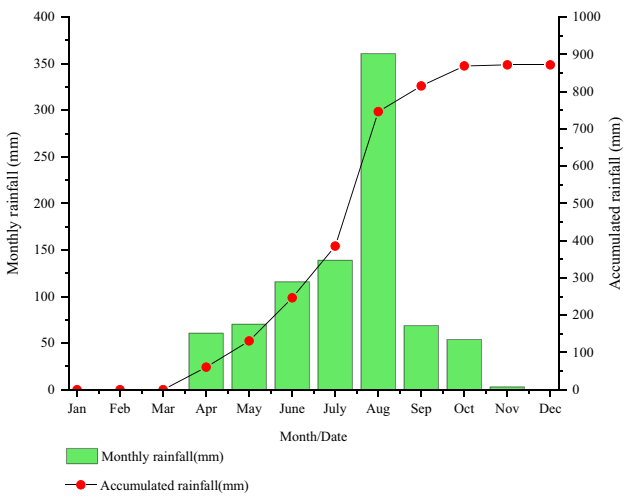

Fig. 3 Distribution of monthly average rainfall

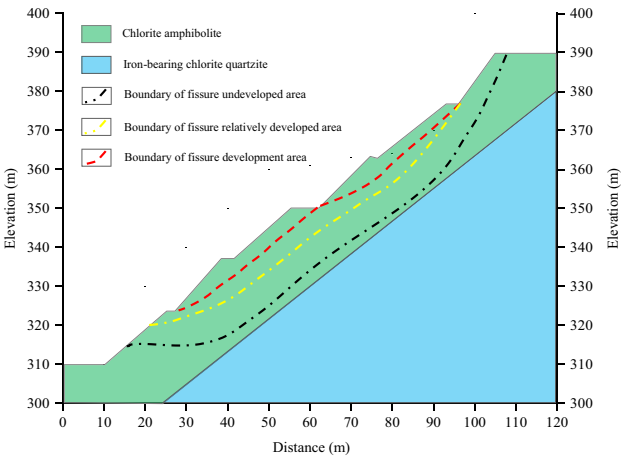

Fig. 4 Engineering geological profile of footwall slope of Nanfen open-pit mine (elevation: 300–390 m)

reduce the strength of rock and soil, which is not conducive to the stability of the slope. The footwall slope of Nanfen open-pit mine has developed fissures. The seepage field of fissured rock mass changes greatly under extreme rainfall conditions, which affects the slope stability; with the continuous rainfall, the continuous softening effect of water on rock of the slope also reduces the slope stability.

Table 1 Statistics on rainfall and landslides in Nanfen open-pit mine (two-year cumulative value of each month from November 2010 to November 2012)

Month	January	February	March	April	May	June	July	August	September	October	November	December
Days of rain	0	0	0	18	11	38	30	37	25	26	3	0
Days of heavy rain (More than 50 mm within 24 h)	0	0	0	0	2	6	8	9	9	4	0	0
Number of landslides	1	0	0	0	0	4	6	15	2	2	0	0

Numerical Simulation

It is found that extreme rainfall is an important inducing factor of footwall slope landslide in Nanfen open-pit mine. The change of seepage field caused by fissures and the slope instability caused by the softening of rock and soil by rain cannot be ignored. It is necessary to study the influence of fissures on slope rainfall infiltration and analyze the softening of slope rock mass by rainfall.

Numerical Simulation Process

The typical profile of 310–390 m platform of footwall slope of Nanfen open-pit mine was selected as the numerical simulation object to simulate the rainfall infiltration and softening of fissured soft rock slope. Using seep/W and sigma/W numerical simulation software based on finite element method, 22 groups of slope rainfall seepage numerical models with different fissure depths, different fissure angles, different fissure spacing and different permeability coefficient ratios were established, and three groups of numerical models of slope stability under rainfall conditions were established, including without fissure and softening, with fissure and without softening, with fissure and with softening. The simulation results of pore pressure and displacement were compared and analyzed. The drainage effect of slope drainage holes was simulated and analyzed. The numerical simulation process is shown in Fig. 5.

Numerical Model

Model and Boundary Conditions

In order to study the rainfall seepage and slope stability of the 310–390 m platform of the footwall slope of Nanfen open-pit mine, the numerical model was established with an elevation of 300–390 m and a distance of 120 m. There were four layers of strata from top to bottom within the model, including fissure development area, fissure relatively development area, chlorite amphibolite area and iron-bearing chlorite quartzite. According to the geological survey report [50], the seepage parameters and mechanical parameters of the model are shown in Tables 2 and 3. Twenty-two groups of numerical models under different rainfall seepage conditions and three groups of numerical analysis models of slope stability were established. In the rainfall seepage numerical model, the slope surface was seepage boundary, and the bottom boundary and left and right boundaries were impermeable boundary. The slope stability analysis model adopted the displacement constraint boundary, in which the bottom edge was the displacement fixed boundary, the left and right edges were the horizontal displacement fixed boundary, and the slope surface was the free boundary. Triangular and quadrilateral elements were mixed in the numerical model, with a total of 6157 nodes and 5989 elements, as illustrated in Fig. 6.

Seepage Theory and Parameters

There are pores and fissures on the surface of the slope, and the part above the groundwater level is in an unsaturated state. The permeability coefficient of unsaturated zone is often less than that of saturated zone, when the water content decreases, the flowing water decreases. In the unsaturated seepage stress analysis, the slope is regarded as a porous medium, the gas in the porous medium is regarded as an ideal gas, and the internal fluid follows Darcy's seepage law [51]. Therefore, in the unsaturated seepage analysis of soft rock slope, Richards's governing equation is used to express the permeability coefficient of unsaturated zone as a function related to saturation, matrix suction or volume water content:

$$m_w \rho_w g \frac{\partial H_w}{\partial t} - \frac{\partial}{\partial x}\left(k_x \frac{\partial H_w}{\partial x}\right) - \frac{\partial}{\partial y}\left(k_y \frac{\partial H_w}{\partial y}\right) = 0 \quad (1)$$

where $m_w = \frac{\partial \theta_w}{\partial u_w}$ is the slope of water cut characteristic curve, which represents the change rate of water content of rock mass with pore water pressure, H_w is the unsaturated total head, θ_w is the volume moisture content, u_w is pore water pressure, ρ_w is the density of water, g is gravity, and k_x and k_y are permeability coefficients in x and y directions, respectively. The relationship between permeability coefficient and matrix suction (SWCC) could be expressed as:

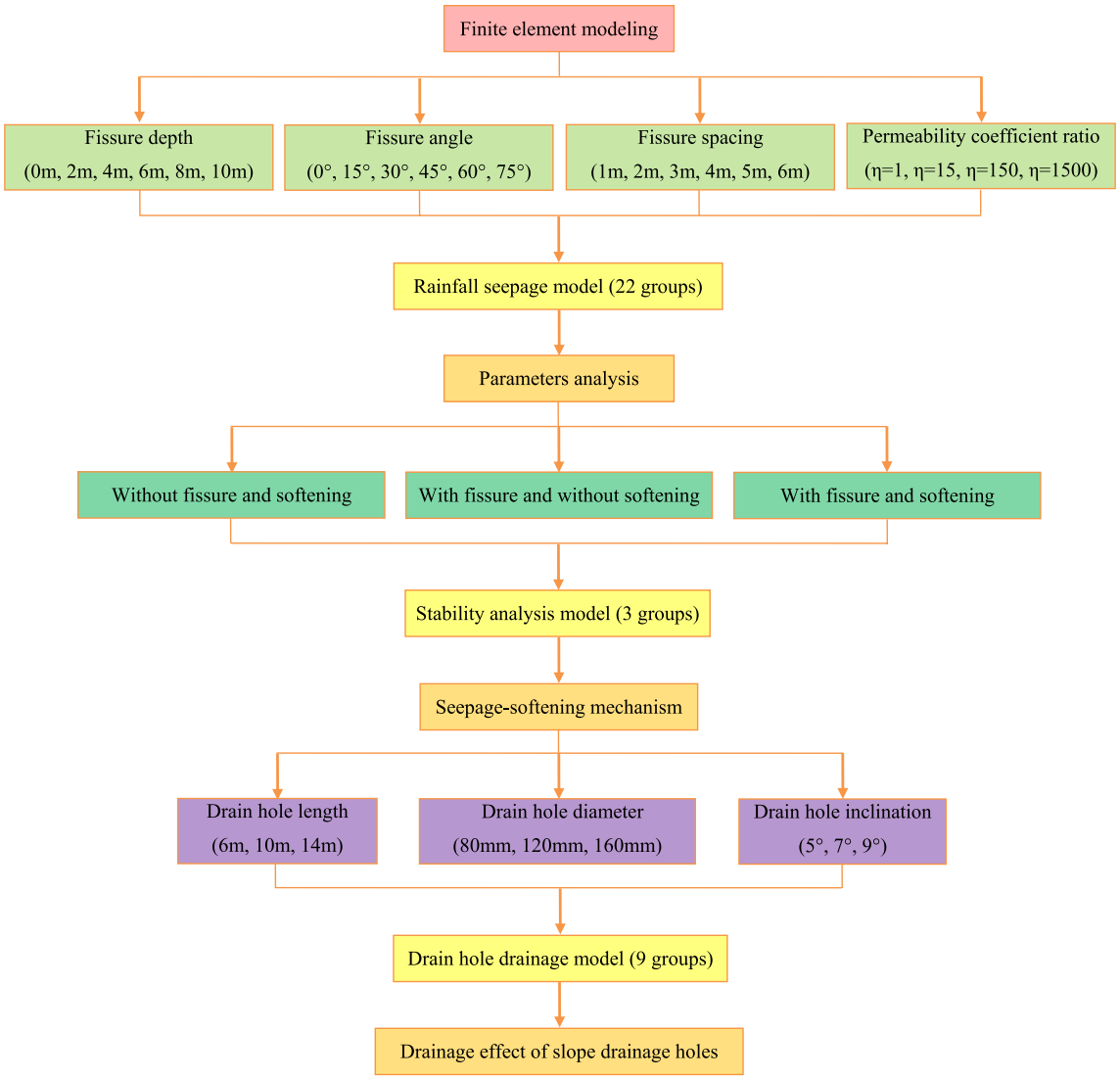

Fig. 5 Numerical simulation process

Table 2 Seepage parameters of the model

Stratum	Saturated water content θ_s	Residual water content θ_r	Model fitting parameters		Saturated permeability coefficient ks (m/s)
			a	n	
Fissure development	0.45	0.16	1.5×10^{-4}	1.06	2.4×10^{-7}
Fissure relatively developed	0.42	0.14	2.1×10^{-3}	1.04	1.8×10^{-7}
Chlorite amphibolite	0.40	0.13	1.5×10^{-2}	1.05	5.6×10^{-8}
Iron-bearing chlorite quartzite	0.37	0.10	1.1×10^{-2}	1.01	1.2×10^{-8}

$$k_w = k_s \frac{[1 - a\psi^{n-1}(1 + (a\psi^n)^{-m})]^2}{(1 + a\psi^n)^{\frac{m}{2}}} \quad (2)$$

where k_s is the saturated permeability coefficient. a, n and m are model fitting parameters, $n = 1/(1\text{-}m)$. Ψ is matrix suction.

Table 3 Mechanical parameters of the model

Stratum	Unit weight (kN/m^3)	Cohesion (kPa)		Internal friction angle (°)		Elastic modulus (MPa)	Poisson' ratio
		Natural state	Saturation 14 d	Natural state	Saturation 14 d		
Fissure development	21.5	45.2	16.1	26.3	23.4	7.3	0.27
Fissure relatively developed	23.3	53.4	19.3	29.9	25.2	8.4	0.25
Chlorite amphibolite	24.1	177.2	53.5	32.2	26.6	17.2	0.23
Iron-bearing chlorite quartzite	24.7	192.8	72.4	37.3	30.1	21.5	0.22

$$\theta_w = \theta_r + \frac{\theta_s - \theta_r}{[1 + (\frac{\Psi}{a})^n]^m} \tag{3}$$

where θ_w is the water content, θ_s is the saturated water content, θ_r is the residual water content, and Ψ is matrix suction. When the saturated permeability coefficient k_s, model fitting parameters a and n, saturated water content θ_s and residual water content θ_r are obtained, the relationship between permeability coefficient and volume water content or matrix suction can be obtained. The seepage parameters of rock and soil mass could be obtained through indoor pressure plate test and on-site double-ring water injection test, as shown in Table 2.

Slope Stability Analysis Theory and Mechanics Parameters

In the calculation of unsaturated soil, the shear strength formula of linear unsaturated soil proposed by Fredlund and Morgenstern [52] was adopted, as shown in Eq. (4).

$$\tau_f = c' + (\sigma - u_a)\tan\phi' + (u_a - u_\omega)\tan\phi^b \tag{4}$$

where c' is effective cohesion, σ is total normal stress on the failure surface,u_a is pore gas pressure on the failure surface, u_ω is pore water pressure on the failure surface, ϕ' is the internal friction angle related to the net normal stress state variable $(\sigma - u_a)$, and ϕ^b is rate of shear strength increasing with matric suction $(u_a - u_\omega)$.

Through geological analysis and field exploration, rock samples were obtained for indoor testing, as shown in Fig. 7. Mechanical parameter testing was performed on samples in their natural state and those saturated for 14 days. The cohesive value depended on the density of rock joints and the cohesive of intact rock blocks. After obtaining relevant test data of the samples, the value of cohesive was calculated using empirical formula (5).

$$C = C_I[0.114e^{-0.48(t-2)} + 0.02] \tag{5}$$

where C is cohesion, C_I is cohesive of intact rock blocks, and t is density of rock joints. The friction value is taken as the average of the shear resistance friction angle of the intact rock blocks and the peak friction angle of the joints. The rock and soil parameters of the numerical model are shown in Table 3.

Numerical Simulation of Rainfall Infiltration in Fissured Slope

In the numerical model, the solid element was established to equivalent the fissure, the fissure was defined as another material different from rock and soil, and the length, angle and spacing of the established fissure solid element were changed to simulate the fissure distribution. Permeability

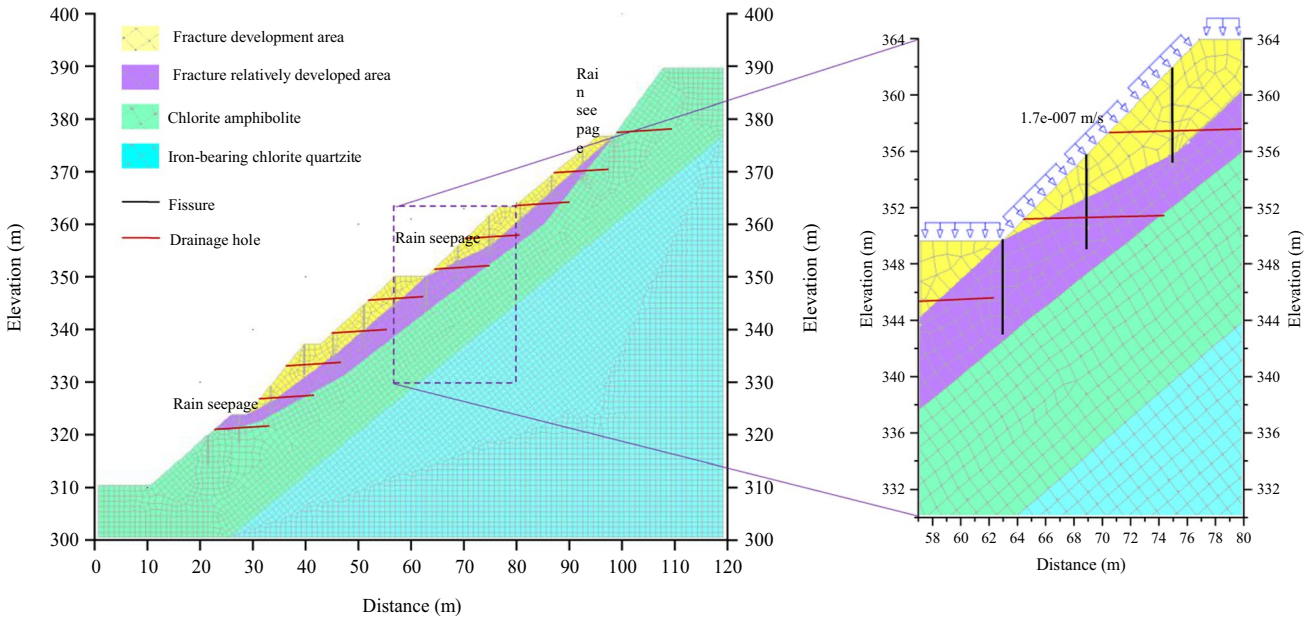

Fig. 6 Numerical model

(a) Field exploration (b) Rock drilling sampling (c) Rock sample testing

Fig. 7 Mechanical parameter testing

coefficient ratio η is the ratio between the permeability coefficient k_y along the fissure direction and the permeability coefficient k_x along the vertical fissure direction [53].

In order to make the numerical simulation close to reality, an extreme rainfall event in August 2011 was simulated. The rainfall was 205 mm and the duration was 14 days, and the cumulative duration of rainfall and rainfall were both the maximum values from November 2010 to November 2012. To study extreme rainfall conditions, this rainfall was selected for simulation. The rainfall intensity was designed as 1.7×10^{-7} m·s^{-1}. Twenty-two groups of cases were designed to simulate the effects of fissure depth, fissure angle, fissure spacing and permeability coefficient ratio on rainfall infiltration process, The numerical simulation scheme is shown in Table 4.

Stability Analysis of Slope Under Seepage and Softening

Under the condition of rainfall infiltration, the change of seepage field will lead to the temporary increase of pore water pressure in soft rock slope, the increase of water content, the decrease of matrix suction, and the transition of soft rock from unsaturated state to saturated state. When the pore water pressure increases to a positive value, the corresponding area in the slope is called transient saturation area, and the rock and soil in the transient saturation zone of the slope will soften.

In this paper, the transient saturation zone of the slope during rainfall was connected with the softening zone of the slope, the soft rock softening parameters measured in

Table 4 Numerical simulation scheme of rainfall seepage

Scheme	Fissure depth (m)	Fissure angle (°)	Fissure spacing (m)	Permeability coefficient ratio η	Rainfall intensity ($m \cdot s^{-1}$)	Rainfall duration (d)
1	0, 2, 4, 6, 8, 10	0	–	1	1.7×10^{-7}	14
2	6	0, 15, 30, 45, 60, 75	–	1		
3	6	0	1, 2, 3, 4, 5, 6	1		
4	6	0	–	1, 15, 150, 1500		

the test were given to the corresponding soft rock mass in the transient saturation zone, and then the water softening region and softening degree of the soft rock slope were simulated by determining the occurrence region and duration of the transient saturation zone, so as to realize the indirect simulation of the softening effect of the soft rock slope. The specific implementation steps are as follows:

1. Calculate the initial in situ stress and initial seepage field of slope stratum.
2. Distribution of slope transient saturation zone at different times is obtained by rainfall infiltration simulation.
3. The water immersion test and analogy estimation of slope rock mass softening in water are carried out to obtain the 14-day saturated mechanical parameter values of slope rock mass as shown in Table 3.
4. The distribution of the transient saturation zone of the slope in (2) corresponds to the softening parameter value of the rock mass in (3).
5. According to step (4), modify the rock mass mechanical parameters in the numerical model at a certain rainfall time.
6. Input the calculation results of seepage field into the numerical model of the certain rainfall time in (5).
7. The slope stability calculation considering the seepage softening effect of soft rock slope is carried out.

Numerical Simulation Results

Influence of Fissures on Rainfall Infiltration

Rainfall Infiltration with Different Fissure Depths

Under different fissure depths, when rainfall lasts for 14 days, the pore water pressure distribution is shown in Fig. 8. The seepage field without fissure was significantly different from that with fissure; with the increased of fissure depth, the depth and range of rainfall infiltration also expanded. When the fissure depth was 2 m, the infiltration depth was 5 m, and when the fissure depth was 10 m, the infiltration influence depth was 20 m. Due to the large permeability coefficient of the fissure, the rainwater first entered the slope fissure; however, due to the small permeability coefficient of the rock and soil mass of the slope, the rainwater in the fissure was not easy to flow in the rock and soil mass, and the rainwater collects in the fissure until the fissure was completely filled. A pressure head almost the same as the fissure depth was formed in the fissure. When the fissure was filled with rainwater, the rainwater in the fissure changed from non-pressure infiltration to pressure infiltration. Therefore, the greater the fissure depth, the greater the pore water pressure and rainfall infiltration depth in the fissure.

The variation curve of pore water pressure with depth under different fissure depths after 14 days of rainfall is shown in Fig. 9. When there was no fissure, the impact of rainfall on pore water pressure was minimal. When the fissure depth was greater than 6 m, the infiltration line under the fissure had coincided with the groundwater level line, and the saturated area increased rapidly and finally directly caused the rise of groundwater level. When the fissure depth was 10 m, the depth of influence reached about 15 m. As the depth of fissures increased, the impact of rainfall on the slope seepage field gradually increased.

Rainfall Infiltration with Different Fissure Angles

Under different fissure angles, when rainfall lasts for 14 days, the pore water pressure distribution is shown in Fig. 10, and the slope distance of the fissure is 68.5 m. It could be seen that with the increase of fissure angle, the infiltration depth and infiltration range gradually decrease. After a long period of rainfall, the fissure gradually reached a saturated state, and its saturated permeability coefficient was greater than the rainfall intensity. In this case, the infiltration process was controlled by the rainfall intensity. The smaller the fissure angle was, the stronger the vertical permeability was, and the rainfall was easier to infiltrate, causing the saturation of the deep area of the slope. When the fissure angle increased, the vertical permeability decreases, the horizontal permeability increased, and the rainwater was easy to flow horizontally. However, due to the lack of gravity of downward seepage, the infiltration range decreased significantly.

The variation curve of pore water pressure with depth under different fissure angles after 14 days of rainfall is shown in Fig. 11. When the fissure angle was 0°, the fissure

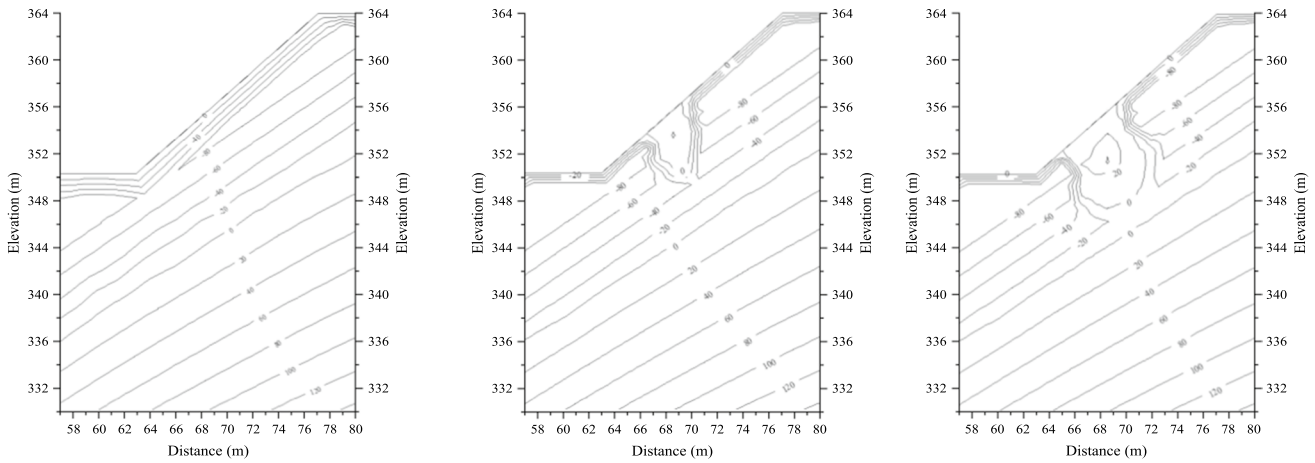

(a) Fissure depth 0 m (b) Fissure depth 2 m (c) Fissure depth 4 m

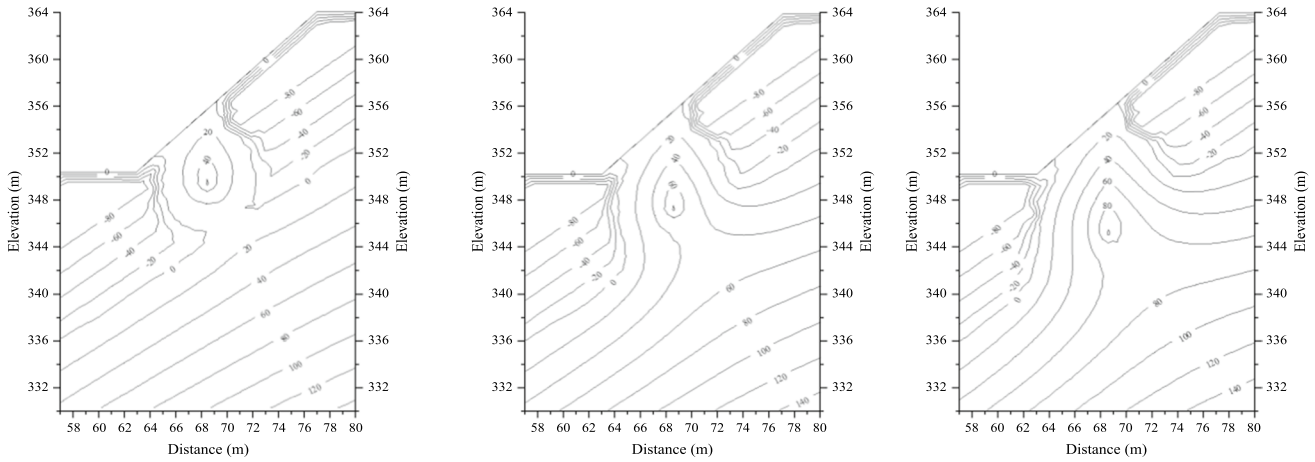

(d)Fissure depth 6 m (e) Fissure depth 8 m (f) Fissure depth 10 m

Fig. 8 Pore water pressure distribution at different fissure depths (unit: kPa)

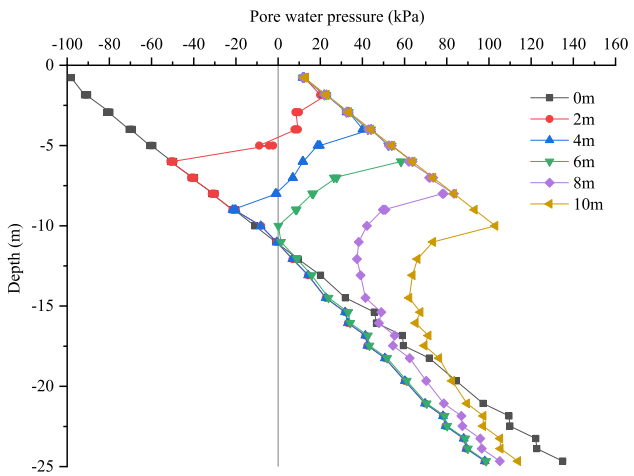

Fig. 9 Pore water pressure with depth under different fissure depths

affected the seepage depth of about 7 m, and all above the groundwater level were saturated. As the fissure angle increased, the depth of influence gradually decreased and the unsaturated depth gradually increased. After an fissure angle of 30°, an unsaturated region appeared. When the fissure angle was greater than 75°, the depth of the surface saturated area was about 2.5 m, and the variation of the slope seepage field was relatively small.

Rainfall Infiltration with Different Fissure Spacing

Under different fissure spacing, when rainfall lasts for 14 days, the pore water pressure distribution is shown in Fig. 12. When the fissure spacing was small, the saturated areas in the slope were connected with each other. With

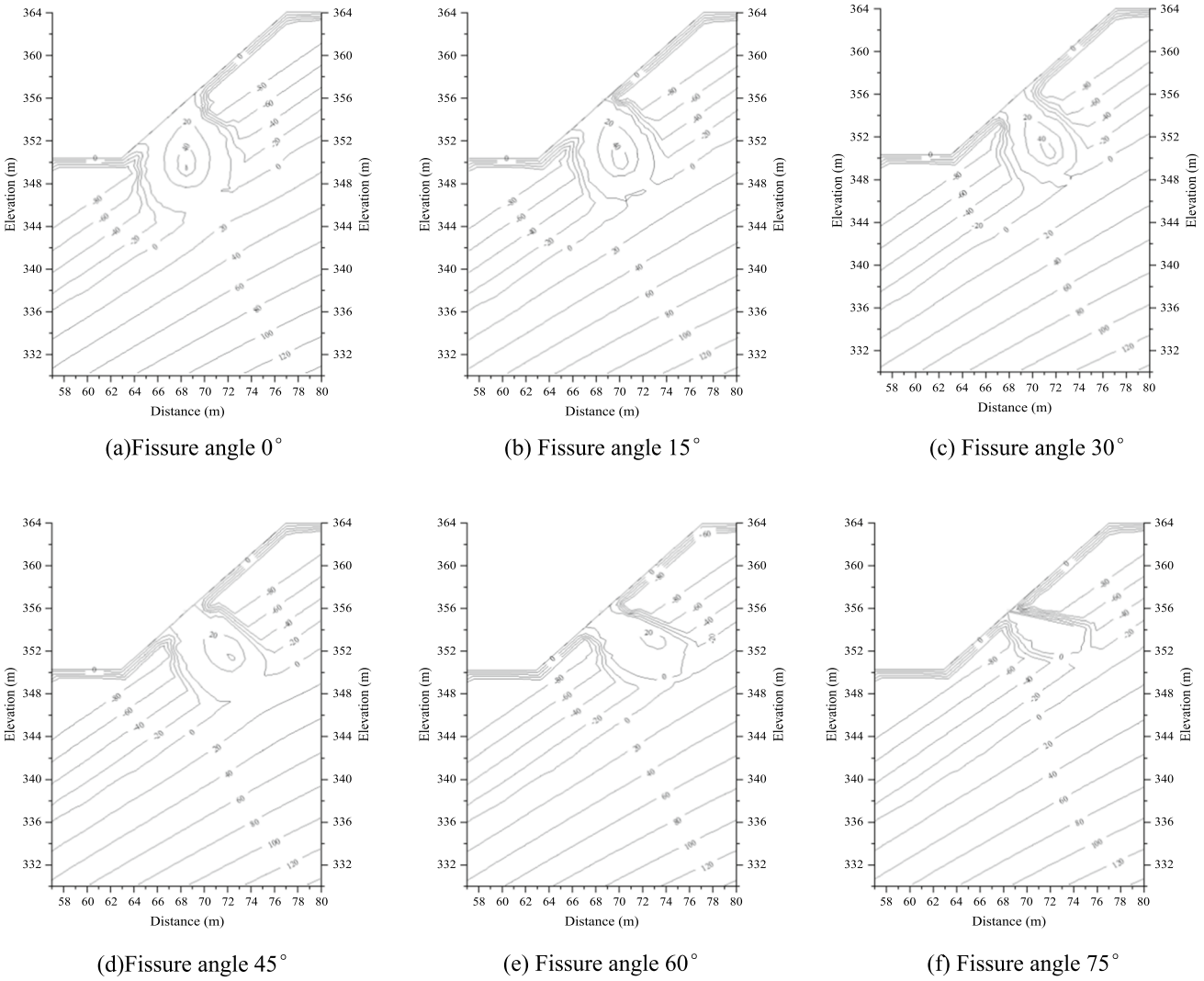

Fig. 10 Pore water pressure distribution at different fissure angles (unit: kPa)

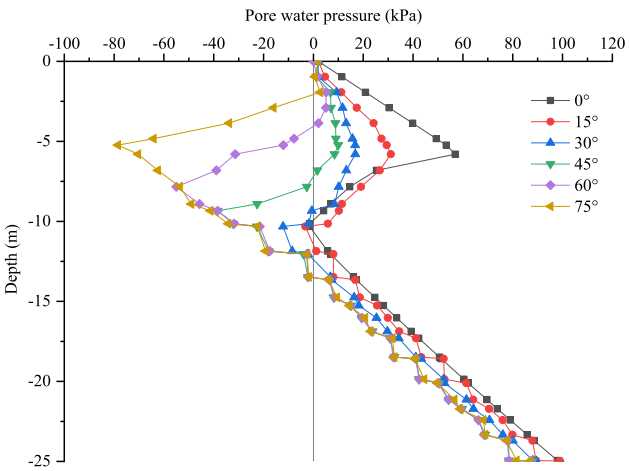

Fig. 11 Pore water pressure with depth under different fissure angles

the increased of fissure spacing, the saturated positive pore water pressure area was gradually separated. When the fissure spacing was greater than 4 m, there was an unsaturated area with negative pressure between the fissures.

The variation curve of pore water pressure with depth under different fissure spacing after 14 days of rainfall is shown in Fig. 13. There was no significant change in rainfall infiltration depth between 1 and 6 m fissure spacing. With the increased of fissure spacing, the positive value of pore water pressure gradually decreased, indicating that the larger the fissure spacing was, the lower the saturation range would be. When the fissure spacing was small and the fissure density was large, the affected area of rainwater infiltration will further increased, which was unfavorable to the slope stability.

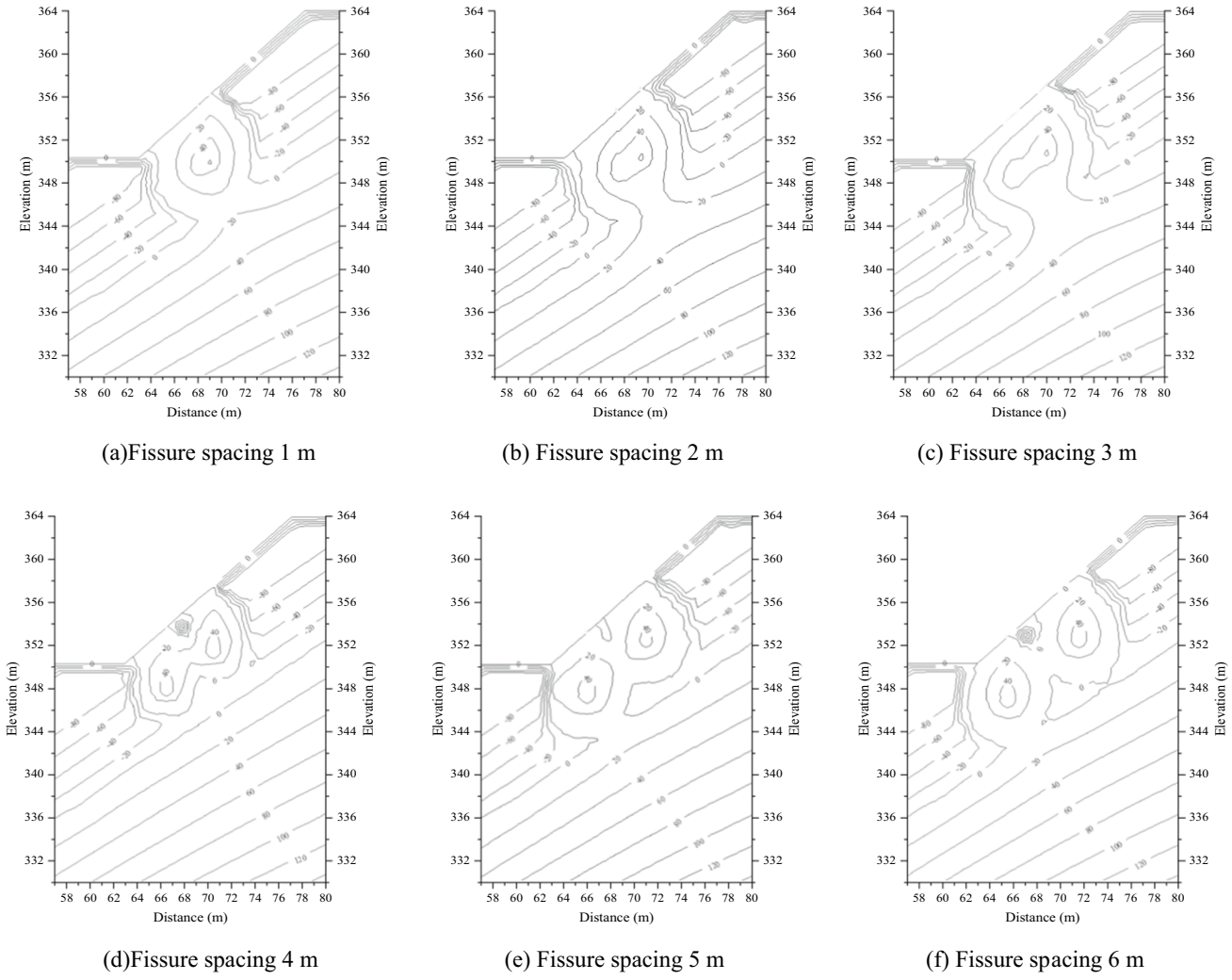

(a)Fissure spacing 1 m (b) Fissure spacing 2 m (c) Fissure spacing 3 m

(d)Fissure spacing 4 m (e) Fissure spacing 5 m (f) Fissure spacing 6 m

Fig. 12 Pore water pressure distribution at different fissure spacing (unit: kPa)

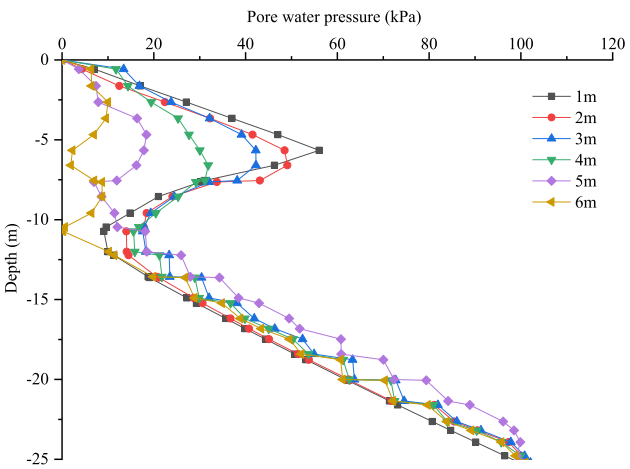

Fig.13 Pore water pressure with depth under different fissure spacing

Rainfall Infiltration Under Different Permeability Coefficient Ratio

Under different permeability coefficient ratio η, when rainfall lasts for 14 days, the pore water pressure distribution is shown in Fig. 14. With the increased of permeability coefficient ratio, the vertical permeability coefficient in the fissure increased significantly, the fissure was saturated rapidly, and the permeability coefficient also increased from unsaturated permeability coefficient to saturated permeability coefficient, which was greater than the rainfall intensity. When the permeability coefficient ratio was greater than 10, there was a saturation zone near the fissure, the maximum pore water pressure was more than 40 kPa, the saturation line quickly coincided with the groundwater level line, the saturation range inside the slope increased, the groundwater level line

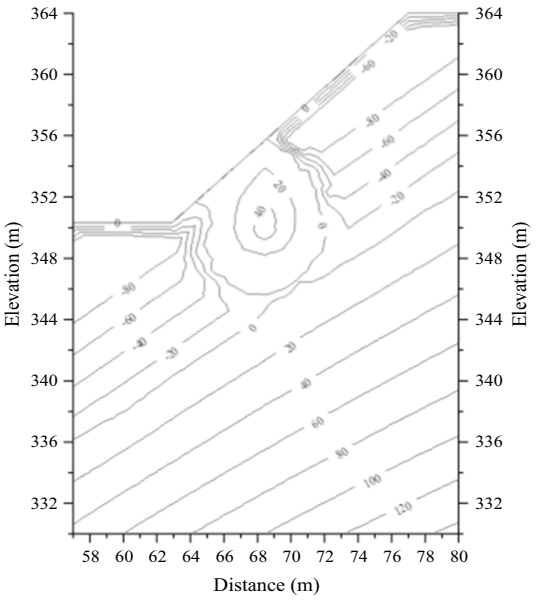

(a)Permeability coefficient ratio η=1

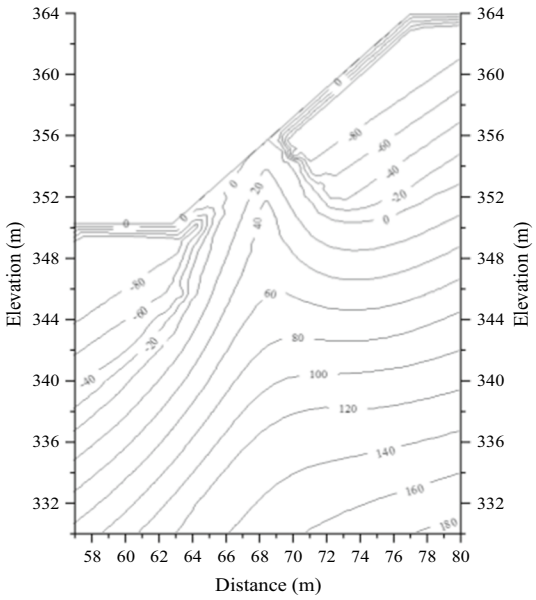

(b) Permeability coefficient ratio η=15

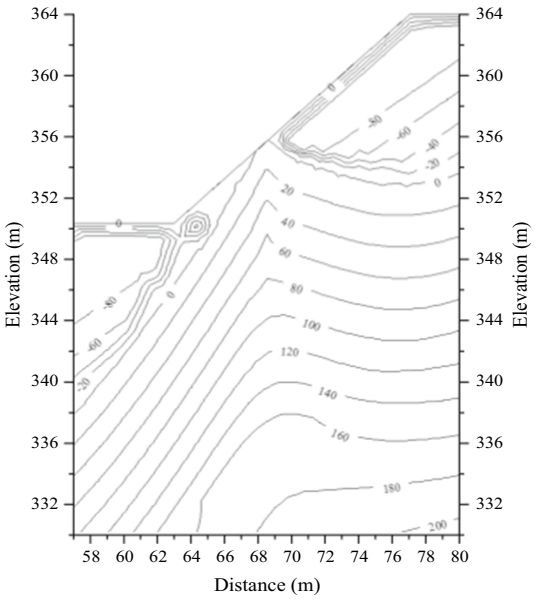

(a)Permeability coefficient ratio η=150

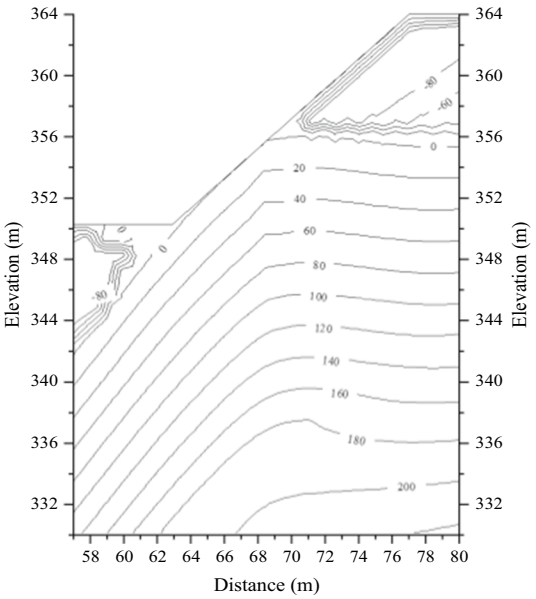

(b) Permeability coefficient ratio η=1500

Fig. 14 Pore water pressure distribution at different fissure permeability coefficient ratios (unit: kPa)

rose to the surface, and the saturation area on the slope surface expanded.

The variation curve of pore water pressure with depth under different permeability coefficient ratios after 14 days of rainfall is shown in Fig. 15. When the permeability coefficient ratio was 1 and 15, the pore water pressure decreased and then increased with increasing depth. When the permeability coefficient ratio was 150 and 1500, the pore water pressure increased with the depth within the fissure range, indicating that a large amount of rainfall flowed into the slope, the phreatic line was connected with the groundwater level line, the water level line rose, and the pore water pressure increased.

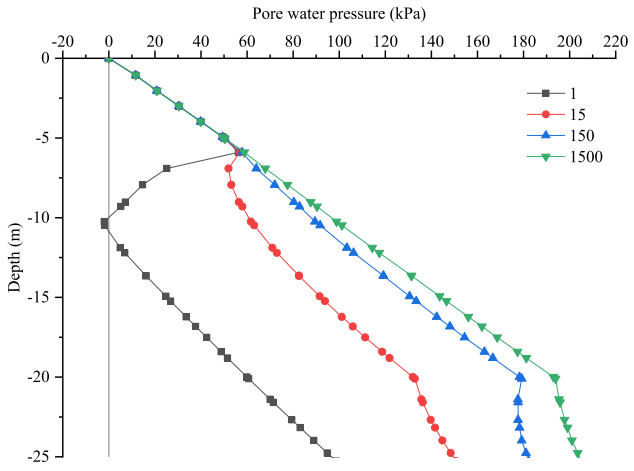

Fig. 15 Pore water pressure with depth under different fissure permeability coefficient ratios

Influence of Rock Mass Fissure and Softening on Slope Stability Under Extreme Rainfall

In order to study the influence of fissure and water softening factors of rock and soil mass on slope stability under extreme rainfall, the numerical models of slope stability without fissure and softening, with fissure and without softening, and with fissure and with softening under rainfall conditions were established. For the scheme with fissures and softening, the stability analysis of slope seepage and softening was carried out according to the method proposed in "Stability Analysis of Slope Under Seepage and Softening" section. There were three groups of slope stability calculation schemes designed in this paper, including without fissure and softening, with fissure and without softening, with fissure and with softening. The detailed scheme is shown in Table 5.

Through numerical analysis, the slope displacement field of 14-d rainfall under different simulation schemes was obtained, as shown in Fig. 16. When fissures and rock softening were not considered (Fig. 16a), the area with large slope displacement was located at 324–338 m steps, and the maximum displacement was 0.048 m. When there were fissures but without softening (Fig. 16b), the area with large slope displacement was located at 324–378 m steps, the maximum displacement was at 360 m elevation, and the displacement was 0.366 m. When there were fissures and the rock mass softening (Fig. 16c), the area with large slope displacement was located at 324–378 m steps, the maximum displacement was at the elevation of 360 m, and the displacement value was 0.615 m. It could be seen that after considering the factors of fissure and rock mass softening, the potential sliding surface of the slope gradually deepened and the scope of potential landslide expanded. The actual failure range and shape of landslide were consistent with the simulation results, indicating the rationality and accuracy of the simulation results.

The curve of slope safety factor with rainfall duration of 14 days is shown in Fig. 17. It could be seen that there was no significant change in the slope safety factor without considering fissures and rock mass softening under rainfall conditions. When there were fissures but no rock softening, the slope safety factor decreased from 1.48 to 1.15. When there were fissures and rock softening, the safety factor of the slope decreased from 1.48 to 0.96 after 10 days of rainfall, and to 0.79 after 14 days of rainfall. The slope safety factor two days before rainfall was mainly affected by the effect of fissure seepage, with the progressed of rainfall, the rock mass in the slope softened when encountering water, and then the slope safety factor was affected by the dual factors of fissure seepage and rock mass softening. When the rainfall lasted for 5 days, the slope safety factor caused by softening decreased to 0.15, and the slope stability factor decreased by 0.1 due to the effect of fissure seepage. The impact of softening on slope stability began to exceed that of fissure seepage. When the rainfall reached 14 days, the safety factor decreased by 0.36 due to softening and 0.3 due to fissure seepage.

Simulation of Drainage Effect of Slope Drainage Holes

Simulation Scheme

This above research confirms that the change of seepage field caused by rainfall infiltration in the early stage of rainfall is an important factor for slope instability; with rainfall infiltration, the softening of slope rock and soil by rainwater

Table 5 Numerical simulation scheme of stability analysis

Scheme	Fissure depth (m)	Fissure angle (°)	Fissure spacing (m)	Permeability coefficient ratio η	Rainfall intensity ($m \cdot s^{-1}$)	Rainfall duration (d)	Soften
1	without				1.7×10^{-7}	14	Without
2	6	0	6	1			Without
3	6	0	6	1			With

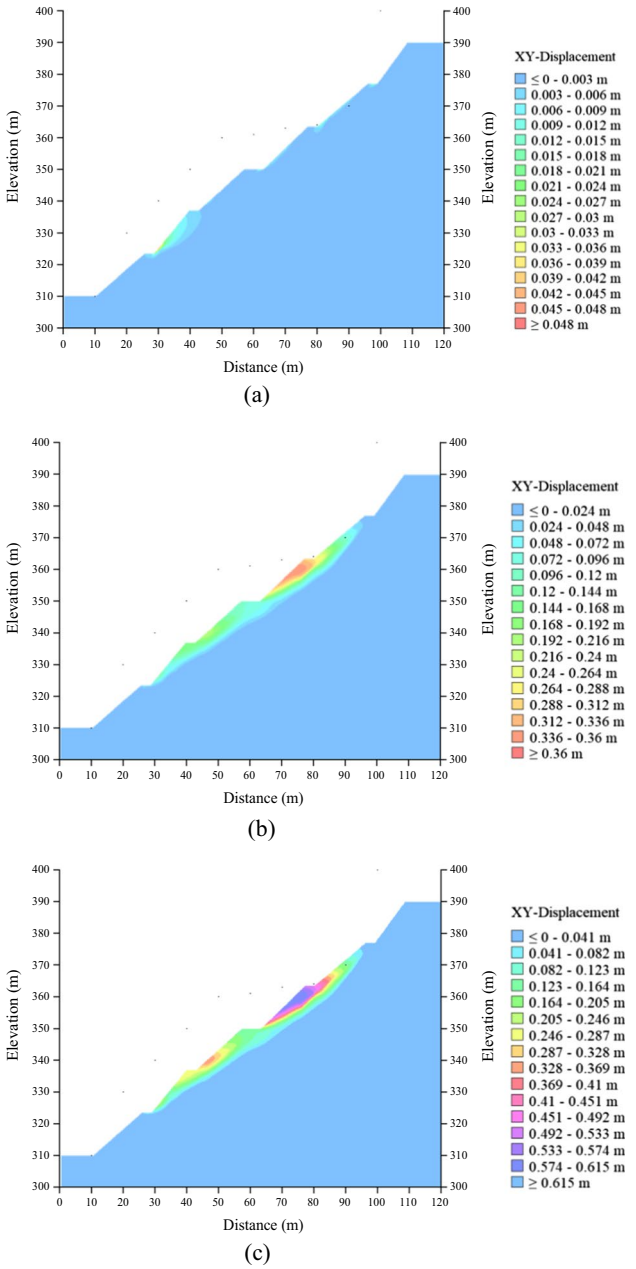

Fig. 16 Numerical results of slope displacement after 14 days of rainfall: **a** Without fissure and softening; **b** With fissure and without softening; **c** With fissure and softening

immersion has become an important factor for the decline of slope safety factor. In order to ensure the stability of the slope under rainfall and the smooth progress of open-pit mining activities, effectively discharging the surface and internal water of the slope is an important goal of slope landslide prevention engineering.

Taking the slope of Nanfen open-pit mine as the research object, the influence of drainage holes on the stability of

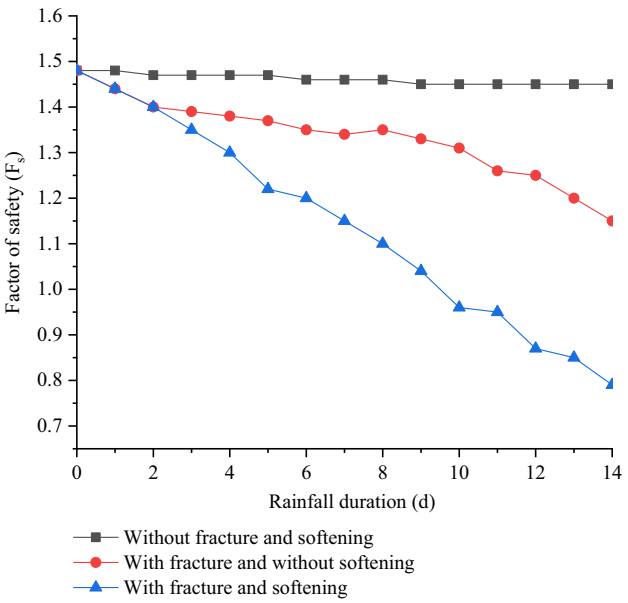

Fig. 17 Curve of slope safety factor with rainfall duration of 14 days

rainfall slope was studied. The numerical model for stability analysis was described in "Numerical Model" section, and the mechanics parameters and simulation methods were described in "Stability Analysis of Slope Under Seepage and Softening" section. Simulated rainfall intensity was 1.7×10^{-7} m·s^{-1}, the rainfall duration was 14 d, the fissure depth of the slope rock mass was 6 m, the fissure angle was 0°, and the fissure spacing was 6. The arrangement of drain holes in the numerical model is shown in Fig. 6. The air element method was used to simulate the drain holes. The hydraulic conductivity of the drainage hole depended on the ratio Q of the permeability coefficient between the drainage hole and the surrounding stratum [54], and the Q value in the simulation was 1000. Table 6 shows the permeability coefficients of drainage holes in different stratum.

The pore water pressure and safety factor under different rainfall time were obtained by simulating the two cases of without drainage holes and with drainage holes. The changes of pore water pressure and safety factor under the two conditions were compared, and the effect of drainage holes on reducing the pore water pressure of slope under extreme rainfall was analyzed.

Seepage Simulation Results

Without drainage holes, the pore water pressure changed obtained from 14d rainfall infiltration simulation of the slope, as shown in Fig. 18. After 4 days of continuous rainfall, water would accumulated on the slope. As the

Table 6 Permeability coefficients of drainage hole

Stratum	Fissure development	Fissure relatively developed	Chlorite amphibolite	Iron-bearing chlorite quartzite
Permeability coefficient (m/s)	2.4×10^{-4}	1.8×10^{-4}	5.6×10^{-5}	1.2×10^{-5}

accumulated water continues to increased, the water level in the soil layer would also rise. After 12 days of continuous rainfall, the water level would rise to a height of 330 m.

When an inclined drain hole with a length of 10 m, a diameter of 80 mm and a dip angle of 5° was arranged on the slope (Fig. 6), the rainfall seepage simulation results are shown in Fig. 19. It could be seen from the figure that after the drainage holes were arranged, the transient saturation area of the slope surface was significantly reduced under rainfall, the rising speed of groundwater level was slowed down, and no obvious ponding area was formed on the slope surface. The groundwater level near the drainage hole was funnel-shaped, the pore water pressure contour near the drainage hole was sparse, and the pore water pressure in the slope body decreased significantly.

Calculation Results of Slope Safety Factor

The slope safety factors without and with drainage holes are shown in Fig. 20. Under continuous heavy rainfall, the safety factor of the slope without drainage holes dropped rapidly. At the initial moment, the safety factor of the slope was 1.48; after 14 days, the safety factor of the slope dropped to 0.79, with a decrease of about 46.6%. The safety factor of the slope without drainage holes was small, which was prone to instability and collapse. After the drainage holes were arranged, the safety factor decreased monotonously in the rainfall process. The safety factor of the slope decreased to 1.18 in 10 d and 1.11 in 14 d, with a decrease of about 25.0%. Compared with the non-drainage hole, the safety factor was increased by 21.6%. The inclined drainage hole could effectively solve the problem of rainfall induced landslide on the slope.

In order to study the influence of drainage hole length, hole diameter and dip angle on slope safety factor, the slope safety factor under different drainage hole parameters at 14-day rainfall was calculated, as shown in Table 7. When the length remained constant, the safety factor increased with the increase of diameters and angles. The diameter and angle remained unchanged, increasing the length would improve the safety factor. By using correlation method to calculate the correlation coefficient between the layout parameters of drainage holes and the slope stability, further conclusions could be drawn that the length and diameter of drainage holes were factors that affect the safety factor.

According to the above analysis, we have drilled holes to arrange drainage pipes to discharge the internal water of the slope; at the same time, we have adopted the method of setting drainage ditches and intercepting ditches to discharge the surface water of the slope. The inclined drain holes are connected with the drainage ditches to form the drainage system of footwall slope in Nanfen open-pit mine, as shown in Fig. 21.

The footwall slope of Nanfen open-pit mine has developed fissures and complex geological conditions, and rainfall has a great impact on the slope. The surface and internal drainage of the slope can reduce rainwater infiltration and timely discharge the deep rock mass water, which plays a direct and beneficial role in maintaining the stability of the slope. When there is no drainage system, rainfall will form runoff on the surface, and rainwater will penetrate into the slope along the fissures, reducing the strength of rock and soil mass and seriously affecting the stability of the slope. In addition, we have installed rainfall monitoring points and sliding force monitoring points to intelligently monitor the real-time hydrogeological environment of the footwall slope of Nanfen open-pit mine. This monitoring method can comprehensively analyze the slope stability and predict its change [55]. The installation of drainage system, the monitoring and early warning system of rainfall and slope sliding force are of great significance to predict and analyze rainfall induced landslide.

Conclusions

A numerical simulation was conducted on the soft rock slope with developed fractures in the footwall of the Nanfen open-pit iron mine. We explored the influence of fissure parameters on rainfall infiltration and analyzed the impact of fissure seepage and rock softening factors on the stability of soft rock slopes under extreme rainfall conditions. Measures for landslide control were proposed for soft rock slopes with developed fissures under extreme rainfall.

1. Fissure depth, fissure angle, fissure spacing and permeability coefficient ratio all had influence on rainwater infiltration, which was mainly reflected in the influence on infiltration depth, infiltration range and saturated area. The fissure depth was positively correlated with the

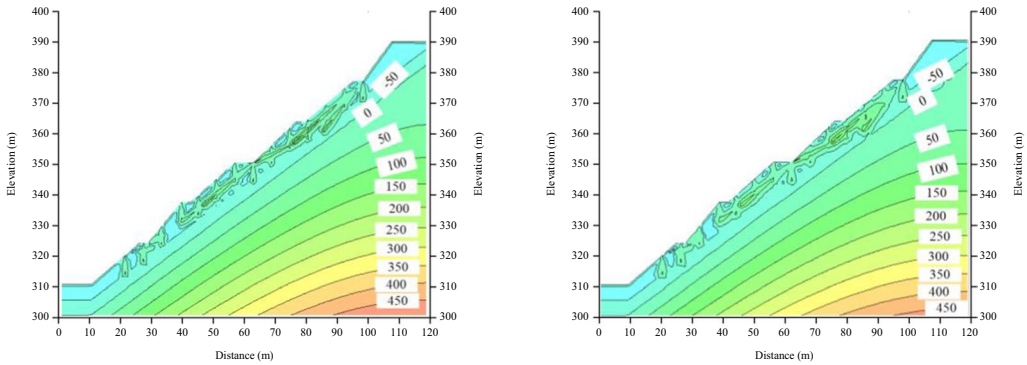

(a) Rainfall duration 1 d

(b) Rainfall duration 2 d

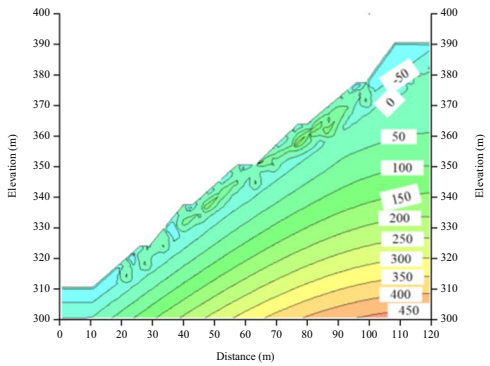

(c) Rainfall duration 4 d

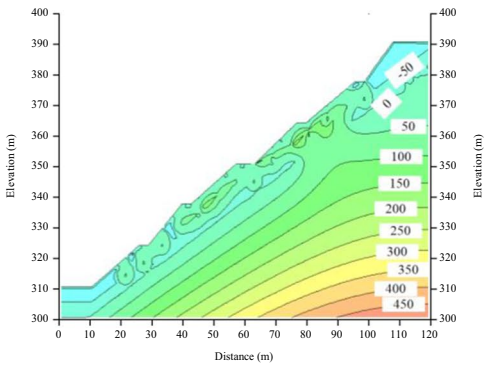

(d) Rainfall duration 6 d

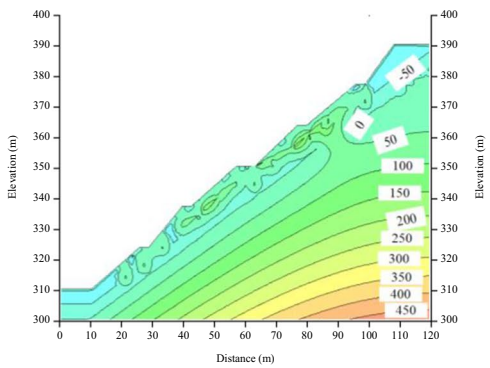

(e) Rainfall duration 8 d

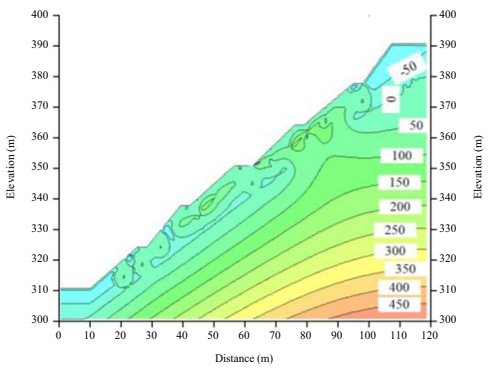

(f) Rainfall duration 10 d

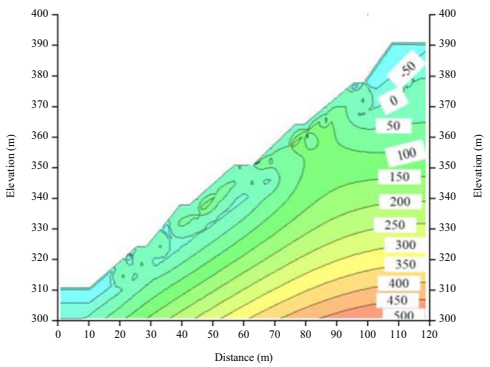

(g) Rainfall duration 12 d

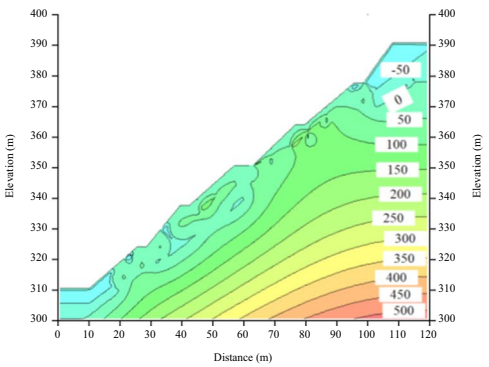

(h) Rainfall duration 14 d

Fig. 18 Pore water pressure of slope during rainfall without drainage hole (unit: kPa)

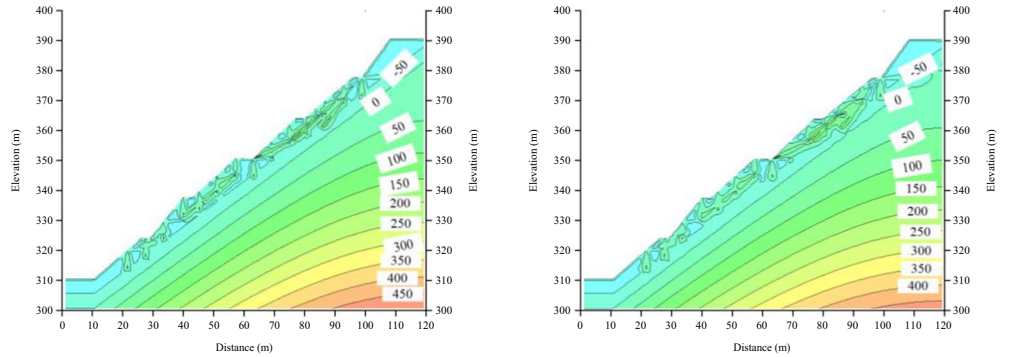

(a) Rainfall duration 1 d

(b) Rainfall duration 2 d

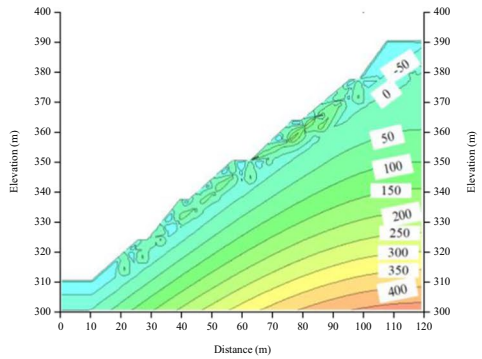

(c) Rainfall duration 4 d

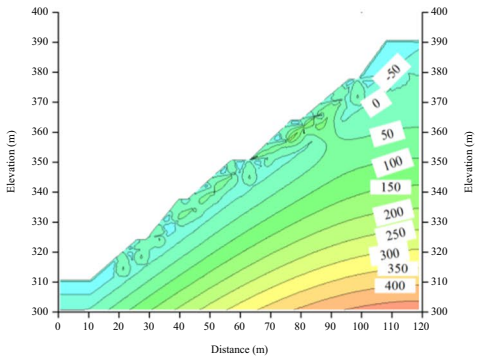

(d) Rainfall duration 6 d

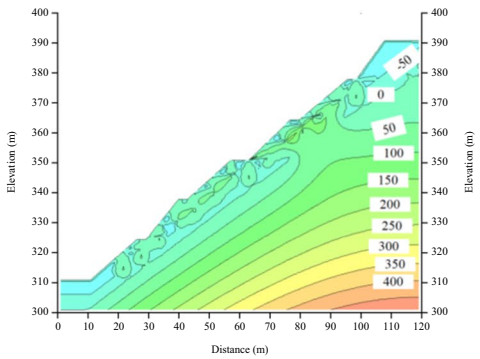

(e) Rainfall duration 8 d

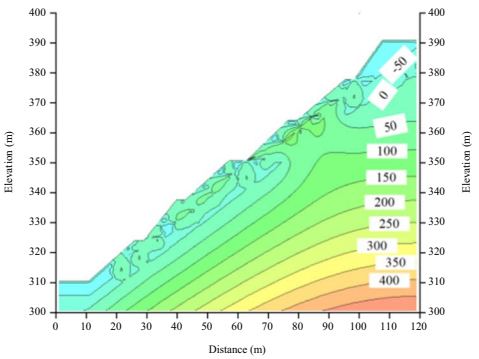

(f) Rainfall duration 10 d

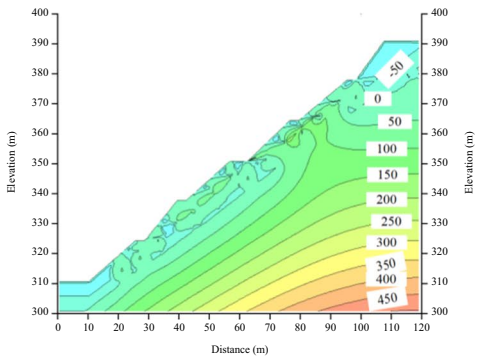

(g) Rainfall duration 12 d

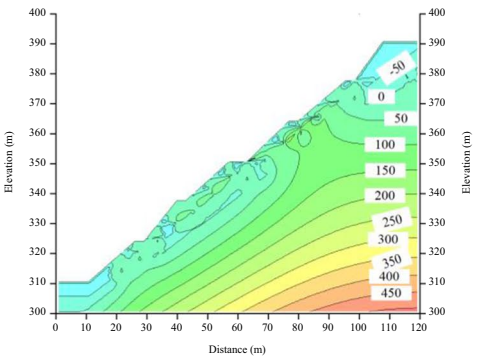

(h) Rainfall duration 14 d

Fig. 19 Pore water pressure of slope during rainfall after arrangement of inclined drainage holes (unit: kPa)

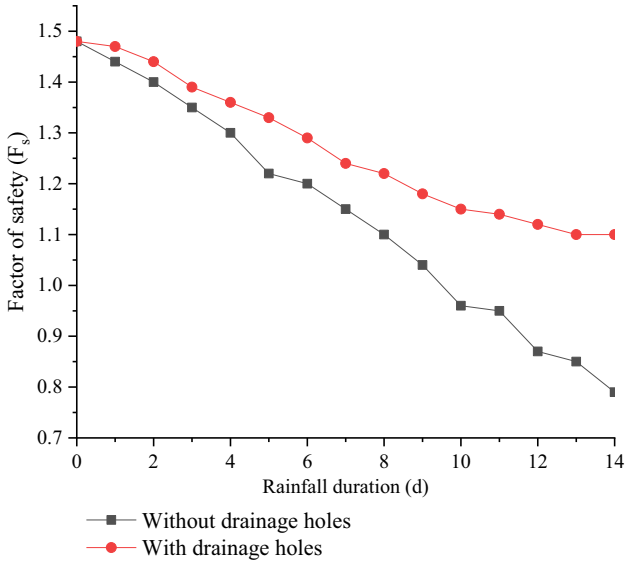

Fig. 20 Slope safety factor without drain hole and with drain hole

Table 7 Slope safety factor under different drainage hole parameters

Scheme	Hole length (m)	Hole diameter (mm)	Dip angle of hole (°)	Safety factor
1	6	80	5	1.04
2	6	120	7	1.05
3	6	160	9	1.06
4	10	80	5	1.11
5	10	120	7	1.12
6	10	160	9	1.14
7	14	80	5	1.18
8	14	120	7	1.19
9	14	160	9	1.19

rainfall infiltration depth and range, the fissure angle was negatively correlated with the rainfall infiltration depth, the fissure spacing was negatively correlated with the rainfall infiltration range and the saturated area size, and the permeability coefficient ratio was positively related to the vertical permeability of rainfall.

2. With the continuation of extreme rainfall, the shallow soft rock of the slope gradually changed from unsaturated state to saturated state, and the pore water pressure field presented a positive, negative and positive regional distribution trend from the surface to the inside of the slope. The transient saturation zone first appeared at the top of the slope and gradually extended to the toe of the slope.
3. Under 14 days of extreme rainfall, rock fissure seepage and soft rock softening with water led to the reduction of slope safety factor by 22.3% and 24.2%, respectively. The change of pore water pressure caused by seepage in the early stage of rainfall had a great impact on the slope stability; with the increased of rainfall duration, the influence of soft rock softening with water on the slope stability gradually increased.
4. Under the inclined drainage holes arranged on the slope (the hole length was 10 m, the hole diameter was 80 mm and the dip angle was 5°), the groundwater level near the drainage holes was funnel-shaped, the contour of the pore water pressure field was sparse and moved to the back edge, and the pore water pressure in the slope significantly reduced. In the process of extreme rainfall, the safety factor of the slope could be kept above 1.11, which was 21.6% higher than that of the non-drainage hole. This showed that the water control method of the inclined drainage hole was an effective means to solve the problem of rainfall induced landslide in soft rock slope with developed fissures.

(a) Surface drainage ditch

(b) Inclined drain holes

Fig. 21 Drainage system of footwall slope in Nanfen open-pit mine

Acknowledgements Financial supports from the Central Guidance on Local Science and Technology Development Fund of Hebei Province under Grant No. 226Z1201G, the Hebei Provincial Higher Education Science and Technology Research Project-Top Young Talents Project under Grant No. BJ2019059, Foundation of Hebei Province for Selected Overseas Scholar under Grant No. C20210109, the Hebei Provincial Natural Science Foundation of China under Grant No. A2021409004, Project for Young Top Talents of Langfang City under Grant No. LFBJ202008 and Ph. D Foundation Project of North China Institute of Aerospace Engineering under Grant No. BKY-2018-21 are gratefully acknowledged.

Data Availability The data used to support the findings of this study are included within the paper.

Declarations

Conflict of interest The authors declare that there is no conflict of interests regarding the publication of this paper.

References

1. Fu HY, Zeng L, Wang GY, Jiang ZM, Yang QX (2012) Stability analysis of soft rock slope under rainfall infiltration. Rock Soil Mech 33(8):2359–2365
2. Zhai Q, Rahardjo H, Satyanaga A, Dai GL (2019) Role of the pore-size distribution function on water flow in unsaturated soil. J Zhejiang Univ Sci A 20:10–20
3. Zhang JM, Luo Y, Zhou Z, Chikhotkin V, Yuan C, Wang SF (2020) Evolution law of cracks based on full-scale model test of slope. J Cent South Univ (Sci Technol) 51(4):1037–1048
4. Liu HQ, Yang JH, Diao YF, Lei TW, Rahma AE (2021) The hydrodynamic mechanism of rainfall runoff from loess slopes treated with incorporated straw. Land Degrad Dev 32(14):3812–3822
5. Su YY, Zhang Y, Wang HY, Lei N, Li P, Wang J (2022) Interactive effects of rainfall intensity and initial thaw depth on slope erosion. Sustainability 14(6):1–14
6. Sheng JC, Li FB, Yao DS, Huang FQ, Song HB, Zhan ML (2012) Experimental study of seepage properties in rocks fracture under coupled hydro-mechano-chemical process. Chin J Rock Mech Eng 31(5):1016–1025
7. Yuan JP, Lin YL, Peng D, Han CL (2016) Influence of anisotropy induced by fractures on rainfall infiltration of slopes. Chin J Geotech Eng 38(1):76–82
8. Xie JR, Zhou CY, Cheng Y (2014) Method of seepage-softening analysis and disaster mechanism in soft rock slope under rainfall. Rock Soil Mech 31(1):197–210
9. Liu J, Zeng L, Fu HY, Shi ZN, Zhang YJ (2019) Variation law of rainfall infiltration depth and saturation zone of soil slope. J Cent South Univ (Sci Technol) 50(2):452–459
10. Cho SE (2016) Stability Analysis of unsaturated soil slopes considering water-air flow caused by rainfall infiltration. Eng Geol 211:184–197
11. Chen GY, He P, Wang G, Sun SQ (2021) Shallow layer destruction law of expansive soil slope under rainfall and the application of geogrid reinforcement. Geofluids 2021(1):1–14
12. Kumar VS, Chandrasekaran SS (2022) Analysis of failure of high slope subjected to rainfall infiltration at Peringavu in Kerala, India. Eng Fail Anal 138:1–31
13. Rahardjo H, Nio AS, Harnas FR, Leong EC (2014) Comprehensive instrumentation for real time monitoring of flux boundary conditions in slope. Proc Earth Planet Sci 9:23–43
14. Rahardjo H, Satyanaga A, Leng EC (2016) Effects of rainfall characteristics on the stability of tropical residual soil slope. E3S Web Conf 9:1–6
15. Zhou JF, Wang JX, Chen W (2014) Lower bound analysis of slope stability subjected to transient unsaturated seepage. Chin J Geotech Eng 36(12):2300–2305
16. Zhang S, Pei XJ, Huang RQ, Zhang XC, Cheng ZL, Zhang ZD (2019) Model test on seepage characteristics and deformation failure modes of loess fill slope under rainfall. China J Highw Transp 32(9):32–41
17. Pedroso DM (2015) A solution to transient seepage in unsaturated porous media. Comput Methods Appl Mech Eng 285(285):791–816
18. Zuo ZB, Zhang LL, Wang JH (2015) Model tests on rainfall-induced colluvium landslides: effects of particle-size distribution. Chin J Geotech Eng 37(7):1319–1327
19. Shi ZN, Qi SX, Fu HY, Zeng L, He ZM, Fang RM (2020) A study of water content distribution and shallow stability of earth slopes subject to rainfall infiltration. Rock Soil Mech 41(3):980–988
20. Deng X, Zhang Y, Tang Y (2021) Investigation on slope rainfall threshold surface based on failure probablolity. Chin J Geol Hazard Control 32(3):70–75
21. Chang ZL, Huang FM, Huang JS, Jiang SH, Zhou CB, Zhu L (2021) Experimental study of the failure mode and mechanism of loess fill slopes induced by rainfall. Eng Geol 280:1–16
22. Liu X, Wang Y (2021) Reliability analysis of an existing slope at a specific site considering rainfall triggering mechanism and its past performance records. Eng Geol 288:1–14
23. Tian DF, Zhang H, Liu DF (2016) 2D FEM numerical simulation of rainfall infiltration for landslide with considering runoff effect and its application. Rock Soil Mech 37(4):1179–1186
24. Bandara S, Ferrarl A, Laloui L (2016) Modelling landslides in unsaturated slopes subjected to rainfall infiltration using material point method. Int J Numer Anal Meth Geomech 40(9):1358–1380
25. Ma JQ, Fu HY, Wang GY, Zeng L, Shi ZN (2018) Seepage characteristics of layered soil slope under rainfall conditions. J Cent South Univ (Sci Technol) 49(2):464–471
26. Long AF, Chen KS, Ji YX (2019) Experimental study on wetting-drying cycles of red clay slopes under different rainfall intensities. Chin J Geotech Eng 41(s2):193–196
27. Wu B, Li LD, Xu L, Li XL (2022) Modelling sheet erosion on steep slopes of clay loess soil using a rainfall simulator. Biosys Eng 216:1–12
28. Wang K, Sheng JC, Gao HC, Tian XD, Zhan ML, Luo YL (2020) Study on seepage characteristics of rough crack under coupling of stress-seepage erosion. Rock Soil Mech 41(s1):30–40
29. Duan LL, Deng HF, Qi Y, Li GY, Peng M (2020) Study on the evolution of seepage characteristics of single-fractured limestone under water-rock interaction. Rock Soil Mech 41(11):3671–3679
30. Park JP, Lee KK, Kosakowski G, Berkowitz B (2015) Transport behavior in three-dimensional fracture intersections. Water Resour Res 39(8):472–477
31. Sheng JC, Zhang XX, Jia CL, Du YC, Zhou Q, Zhan ML, Luo YL, He SY (2017) Experimental study on permeability of limestone fractures under temperature changes. Chin J Rock Mech Eng 36(8):1832–1840
32. Zhang JY, Wan LP, Pan HY, Li JL, Luo ZS, Deng HF (2017) Long-term stability analysis of typical bank slopes considering water-rock interaction characteristics. Chin J Geotech Eng 39(10):1851–1858
33. Hou DG, Zhou YY, Zheng XY (2023) Seepage and stability analysis of fissured expansive soil slope under rainfall. Indian Geotech J 53:180–195
34. Leng XL, Wang C, Zhang J, Sheng Q, Cao SL, Chen J (2021) Deformation development mechanism in a loess slope with

seepage fissures subjected to rainfall and traffic load. Front Earth Sci 9:1–15
35. Zhang Y, Li P, Guo QF, Ren FH, Wu X (2020) Research progress of def. 0rmation and failure mechanism in fractured rock mass under hydromechanical coupling. J Harbin Inst Technol 52(6):21–41
36. Guo BH, Cheng T, Chen Y, Jiao F (2019) Seepage characteristic of marble fracture and effect of filling sands. J Hydraul Eng 50(4):59–70
37. Liu CH, Chen CX, Fu SL (2003) Study on seepage characteristics of a single rock fracture under shear stresses. J Rock Mech Eng 22(10):1651–1655
38. Xiong XB, Li B, Jiang YJ, Zhang CH (2010) Flow mechanism test on single rock fracture and its three-dimensional numerical simulation. Chin J Rock Mech Eng 29(11):2230–2238
39. Zhang PS, Hou JQ, Zhao CY, Li TH (2020) Experimental study on seepage characteristics of red sandstone with different confining pressures and different damage degrees. Chin J Rock Mech Eng 39(12):2405–2415
40. Valko P, Economides MJ (1991) Propagation of hydraulically induced fracture-a continum damage mechanics approach. Int J Rock Mech Min Sci Geomech Abstr 31(3):221–229
41. Yan JK, Huang JB, Li HL, Chen L, Zhang YL (2020) Study on instability mechanism of shallow landslide caused by typhoon and heavy rain. J Geomech 26(4):481–491
42. Lu YG, Xiao QH, Cheng JL (2019) Mechanism and prevention of water-sand inrush in soft rock with weakly abundant water: a case study in Shanghai temple mining area. J China Coal Soc 44(10):3154–3163
43. Bai YJ, Ge H, Feng WK, Xu W, Tie YB (2019) Centrifugal tests on geological evolution and sliding process for red-bed soft rock landslide in Wumeng Mountain Area. Chin J Rock Mech Eng 38(s1):3025–3035
44. Yang X, Zhou CY, Liu Z, Su DL, Du ZC (2016) Model tests for failure mechanism of typical soft rock slopes of red beds under rainfall in South China. Chin J Rock Mech Eng 35(3):549–557
45. Xie XS, Chen HS, Xiao XH, Wang J, Zhou JW (2019) Microstructural characteristics and softening mechanism of red-bed soft rock under water-rock interaction condition. J Eng Geol 27(5):966–972
46. Ji HG, Jiang H, Song ZY, Liu ZQ, Tan J, Liu YJ, Wu YF (2018) Analysis on the microstructure evolution and fracture morphology during the softening process of weakly cemented sandstone. J China Coal Soc 43(4):993–999
47. Jiang JD, Chen SS, Xu J, Liu QS (2018) Mechanical properties and energy characteristics of mudstone under different containing moisture states. J China Coal Soc 43(8):2217–2224
48. Picarelli L, Olivares L, Comegna L, Damiano E (2008) Mechanical aspects of flow-like movements in granular and fine grained soils. Rock Mech Rock Eng 41(1):179–197
49. Xin P, Hu L, Wang T, Fan L, Wu SR, Shi JS (2020) The application of displacement-stress synergetic analysis to landslide monitoring: a case study of beipo landslides in Baoji City, Shaanxi Province. Acta Geosci Sin 41(1):37–48
50. Tao ZG, Hou DG, Lv Q (2012) Geological survey and hazard zoning report on the slope of nanfen open pit mine. Beijing: State Key Lab. For Geo-mechanics and Deep Underground Engineering, pp 32–76
51. Genuchten V, Th M (1980) A closed form equation for prediction the hydraulic conductivity of unsaturated soils. Soil Sci Soc Am J 44(5):892–898
52. Fredlund DG, Morgenstern NR, Widger RA (1978) Shear strength of unsaturated soils. Can Geotech J 15(3):313–321
53. Zeng L, Liu J, Zhang JH, Bian HB, Lu WH (2018) Effect of Colluvial soil slope fracture's anisotropy characteristics on rainwater infiltration process. Adv Civ Eng 2018:1–11
54. Wu SC, Wang M, Han LQ, Zhang XL, Liu ZQ, Li YJ (2022) Influence of drainage hole layout parameters on slope stability under rainfall conditions. Metal Ming 550:222–230
55. Yang XJ, Hou DG, Hao ZL, Wang EY (2016) Fuzzy comprehensive caused by underground mining subsidence and its monitoring. Int J Environ Pollut 59(2/3/4):284–301